Superfluids (Wiley, New York, 1950), Vol. I.
[2]D. Shoenberg, *Superconductivity* (Cambridge U. P., London, 1965).
[3]D. C. Baird and B. K. Mukherjee, Phys. Rev. Lett. **21**, 996 (1968); Phys. Rev. B **3**, 1043 (1971).
[4]A. F. Andreev, Zh. Eksp. Teor. Fiz. **54**, 1510 (1968) [Sov. Phys.-JETP **27**, 809 (1968)].
[5]L. Rinderer, Helv. Phys. Acta **29**, 339 (1956).
[6]H. D. Wiederick, B. K. Mukherjee, and D. C. Baird, J. Phys. D **4**, 1365 (1971).
[7]L. Rinderer, Helv. Phys. Acta **32**, 320 (1959).
[8]E. H. Rhoderick and E. M. Wilson, Nature (Lond.) **194**, 1167 (1962).
[9]R. P. Huebener, R. T. Kampwirth, and J. R. Clem, J. Low Temp. Phys. **6**, 275 (1972).
[10]R. P. Huebener and R. T. Kampwirth, Solid State Commun. **10**, 1289 (1972).
[11]R. P. Huebener and R. T. Kampwirth, Phys. Status Solidi A **13**, 255 (1972).
[12]R. P. Huebener and R. T. Kampwirth, in Proceedings of 1972 Applied Superconductivity Conference, Annapolis, Maryland, edited by H. M. Long and W. F. Gauster, (IEEE, New York, 1972), p. 422.
[13]I. Giaever, Phys. Rev. Lett. **15**, 825 (1965); Phys. Rev. Lett. **16**, 460 (1966).
[14]R. P. Huebener, R. T. Kampwirth, and D. E. Gallus, Proceedings of the Thirteenth International Conference on Low-Temperature Physics, Boulder, Colo., 1972 (unpublished).
[15]J. R. Clem (private communication).
[16]J. R. Clem, R. P. Huebener, and D. E. Gallus (unpublished).
[17]R. P. Huebener, R. T. Kampwirth, and V. A. Rowe, Cryogenics **12**, 100 (1972).
[18]M. Ya. Azbel, Zh. Eksp. Teor. Fiz. Pis'ma Red. **10**, 550 (1969) [JETP Lett. **10**, 351 (1969)].
[19]W. W. Webb and R. J. Warburton, Phys. Rev. Lett. **20**, 461 (1968).
[20]J. Meyer and G. v. Minnigerode, Phys. Lett. A **38**, 529 (1972); and in Ref. 14.
[21]G. I. Rochlin, *Proceedings of the Conference on Fluctuations in Superconductors,* edited by W. S. Goree and F. Chilton (Stanford Research Institute, Palo Alto, Calif. (1968).
[22]P. R. Solomon, Phys. Rev. **179**, 475 (1969).
[23]D. K. C. MacDonald, *Noise and Fluctuations*, (Wiley, New York, 1962), p. 82.
[24]A. Van der Ziel, *Fluctuation Phenomena in Semiconductors* (Academic, New York, 1959); Phys. Lett. A **25**, 672 (1967).
[25]C. Heiden, *Habilitationsschrift* (University of Münster, Münster, 1971).

PHYSICAL REVIEW B VOLUME 7, NUMBER 9 1 MAY 1973

Electrical and Structural Properties of Amorphous Metal–Metal-Oxide Systems

J. J. Hauser
Bell Laboratories, Murray Hill, New Jersey 07974
(Received 2 August 1972)

Amorphous mixtures of Al-Al_2O_3, Sn-SnO_2, Ta-Ta_2O_5, and Ni-NiO were sputtered in various concentrations at room temperature. The resistivity was measured as a function of temperature between 1 and 300 °K in three different ways; two-point and four-point contacts in a planar geometry and in a capacitance configuration. The most extensive measurements conducted on the Al-Al_2O_3 and Sn-SnO_2 systems showed that, over nine orders of magnitude in resistance the resistivity could be described by $\rho=\rho_0\, e^{(T_0/T)^{1/n}}$ with $n=4$ over a wide range of compositions in the Al-Al_2O_3 system. This resistivity behavior along with the current's voltage dependence and the ac resistivity measurements indicate that the conduction mechanism in such films may be similar to the thermally activated hopping mechanism described in other amorphous materials.

I. INTRODUCTION

The electrical and structural properties of metal–metal-oxide films have been studied in both limits: high metal concentration or granular films[1] and low metal concentration or cermet films.[2] The conduction mechanism has, however, been studied only at high temperatures and low electric fields[2–5] except in the granular system Ni–SiO_2, which was investigated at high fields and low temperatures.[6] However, little attention has been given to the conduction mechanism at low temperatures in amorphous metal–metal-oxide films. The approach used in the present study was to investigate the properties of certain metal–metal-oxide systems as a function of the oxide concentration starting from the granular-type films and ending with doped oxide films. One may expect that such a continuous approach will permit a better characterization of films which by electron or x-ray diffraction could only be described as amorphous.

From a theoretical point of view, the conduction in such amorphous materials as Ge and Si films or in 3*d* oxides was described by Mott[7] in terms of a phonon-assisted hopping mechanism. This theory was recently recast using percolation theory[8] and predicts that the electrical resistivity (ρ) should vary as $\exp(\text{const}\times T^{-1/4})$. This temperature dependence has been verified for amorphous Ge and Si[7,9–11] in the temperature range 60–300 °K. On the other hand, although this temperature dependence is observed in Fe_2O_3[12] and NiO[13] below 60 °K, it seems to go over to a power law below 10 °K, in agreement with a recent calculation.[14]

Consequently, the functional dependence of the resistivity on temperature depends on the range of temperature over which the data are fitted and for this reason alone it would be interesting to find out whether other amorphous materials behave in the same manner.

II. EXPERIMENTAL PROCEDURE

The metal–metal-oxide films were deposited using the getter-sputtering technique.[1] The target preparation was similar to the one used for the Al–Al_2O_3 system.[1] A powder mixture of the metal and the oxide of the desired concentration is pressed into the form of a button and a metal stem is pressed into the button. The metal–metal-oxide films ranging in thickness between 0.4 and 26 μm were sputtered onto glass substrates at room temperature at rates varying between 40 and 200 Å/min. Certain films were also sputtered on sapphire substrates at 77 °K and kept at this temperature until measured. The Al–Al_2O_3 films with the highest resistivities were sputtered from an Al–Al_2O_3 target containing 40-wt.% Al_2O_3, and although sputtering is usually a steady-state process, that was not the case in this particular experiment. Indeed, the as-pressed target was insulating and in the first half-hour there was a large amount of arcing at the surface of the target which resulted in the formation of a thin conducting peripheral shell. At the end of this period, sputtering proceeded smoothly, but the films became progressively enriched in aluminum. As a consequence, in order to obtain fairly uniform high-resistivity films, the target had to be scraped before each experiment and the film thickness was kept under 5000 Å in each sputtering experiment. Thicker films were obtained by stacking up several films produced according to the above procedure. The resistivity of the films was measured as a function of temperature between 1 and 300 °K in three different ways: a four-point-contact method measuring the voltage drop created by a constant current (as low as 10 nA) in the plane of the film for resistances up to 10^{10} Ω, a two-point-contact method measuring the current (on a Keithley 610C Electrometer) flowing as a result of a constant applied voltage (90 V) for resistances up to 10^{15} Ω, and finally, a capacitance configuration where the current flowing across the film thickness as a result of a fixed applied voltage between two gold electrodes is measured. The latter method permits very high resistivities to be measured at low resistance levels, and was used to determine the voltage dependence of the current and the same method was used in ac measurements where the resistivity and the dielectric constant were measured up to 1 MHz. The susceptibility of certain films was measured on a sensitive ac bridge using two balanced coils which has been previously described.[15] The structure of the films was established by x-ray and electron diffraction experiments.[16]

III. EXPERIMENTAL RESULTS AND DISCUSSION

The structure of all the films studied in the present experiment can be considered as amorphous or possibly as quasiamorphous, as we shall see when the susceptibility experiments are examined. Indeed, the x-ray diffraction showed no resolvable peaks and the electron diffraction consisted at best of very broad diffuse rings which suggest submicroscopic grains with a diameter smaller than 20 Å. An example of such diffuse electron diffractions can be seen for the Al–Al_2O_3 system in Fig. 4 of Ref. 1. It is best at this point to divide the discussion into four parts corresponding to each of the four systems studied. Indeed, as will be shown in the Summary, certain general conclusions can be drawn which apply to all systems, while on the other hand, certain conclusions are only pertinent to a particular metal–metal-oxide system.

A. Al–Al_2O_2

The temperature dependence of the resistivity of Al–Al_2O_3 films, sputtered from a 35-wt.% Al_2O_3 target, has been already shown in a previous study.[15] It is clear from Fig. 5 of Ref. 15, where the log of the resistance is plotted versus $1/T$ for two films with room-temperature resistivities close to 1.3 Ωcm, that the temperature dependence is slower than an exponential. As a matter of fact, these data can be approximated fairly well by a relationship of the form

$$R = R_0 e^{(T_0/T)^{1/4}}. \quad (1)$$

Before comparing various Al–Al_2O_3 films with different Al_2O_3 content, one should define a parameter which is representative of the Al_2O_3 content of the film. As the sputtering process in this particular instance is not a steady-state process, one cannot use the Al_2O_3 content of the target, but instead one can take the room-temperature resistivity of the film as a measure of the Al_2O_3 content of the film (from now on when resistivity is mentioned without further details it must be read as room-temperature resistivity); this point will be further established in the Sn–SnO_2 system. Granular Al–Al_2O_3 films, i.e., films displaying broad diffuse rings indicating Al grains (about 20 Å in diameter) separated by Al_2O_3 boundaries, display room-temperature resistivities below 1 Ωcm. It is very difficult to ascertain the functional form of the temperature dependence of the resistivity in such films (exponential type versus power law) as the resistance ratio [ρ(RT)/ρ(4.2 °K)] for such films is very close

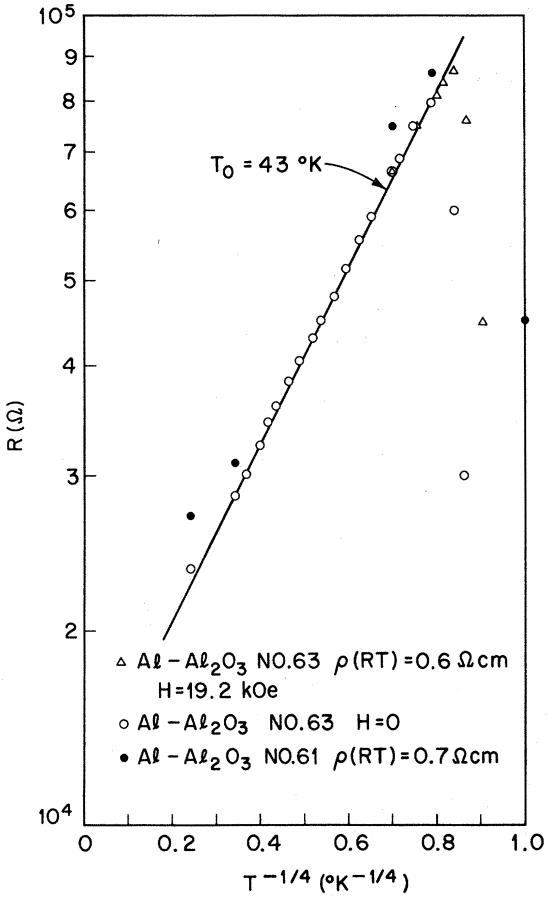

FIG. 1. Temperature dependence of the resistance for two Al–Al_2O_3 films with $\rho(RT) = 0.6$ and 0.7 Ω cm and a superconducting transition around 2.6 °K.

to unity.[1,15] We shall therefore turn our attention to amorphous Al–Al_2O_3 films with $\rho(RT) > 1$ Ω cm. The temperature dependence of the resistivity for all metal–metal-oxide films measured is summarized in Table I. Figure 1 shows the temperature dependence of the resistance for Al–Al_2O_3 films which still display a resistive superconducting transition. The superconducting nature of the transition at 2.6 °K is further demonstrated by the effect of the 19.2-kOe magnetic field which lowers the superconducting transition temperature by about 0.6 °K. Since such films are amorphous as judged by their diffuse electron diffraction patterns, the superconductive resistive transition leads to three distinct structural possibilities: (i) a homogeneous amorphous superconductor, (ii) an inhomogeneous structure consisting of superconducting macroscopic clusters or filaments embedded in a nonsuperconducting amorphous matrix, and (iii) superconducting submicroscopic grains (diameter smaller than 20 Å) separated by Al_2O_3-rich tunnel barriers. The study of the transition temperature as a function of resistivity[1] as well as penetration depth and critical field measurements[15] favor the third possibility. The fact that the resistive transition temperature decreases smoothly above a maximum with increasing resistivity (increasing Al_2O_3 content) as the grain size decreases without any major discontinuity when the electron diffraction becomes totally diffuse is a good argument against an amorphous superconductor. As a matter of fact, no truly glassy superconductor has yet been discovered. The transverse electrical conductivity of the films is quite similar to the planar conductivity, which is a good indication against filamentary inhomogeneities. Besides the fact that sputtering is known to produce very homogeneous films, the fact that films deposited at 77 °K (where diffusion and therefore grain growth does not occur) have similar structure and electrical properties[1,15] to films deposited at room temperature would tend to rule out the possibility of large clusters. Consequently, as the Al_2O_3 content is increased, the resistivity increases and the grain size diminishes (becoming submicroscopic when the electron diffraction pattern is diffuse), but a resistive transi-

TABLE I. Properties of metal–metal-oxide films.

Film		d (Å)	ρ_{RT} (Ω cm)	n	T_0 (°K)
Al–Al_2O_3	No. 63	4800	0.6	4	4.3×10
Al–Al_2O_3	No. 61	4800	0.7	4	4.3×10
Al–Al_2O_3	No. 62	4800	1.5	4	5.5×10^2
Al–Al_2O_3	No. 60	4800	5.05	4	6.1×10^3
Al–Al_2O_3	No. 65	5000	5.5	4	7.7×10^4
Al–Al_2O_3	No. 70	5000	9.7	3	6.2×10^3
Al–Al_2O_3	No. 69	4000	17	2	7×10^2
Al–Al_2O_3	No. 68	3200	35	2	1.1×10^3
Al–Al_2O_3	No. 71	3200	320	1.5	...
Al–Al_2O_3	No. 67	3200	640	1	1.2×10^2 (10 meV)
Al–Al_2O_3	No. 73[a]	...	...	3	2.2×10^4
Sn–SnO_2	No. 25	4370	0.15	1	1.6×10 (1.4 meV)
Sn–SnO_2	No. 16	6050	0.2	1	1.6×10 (1.4 meV)
Sn–SnO_2	No. 20	6550	0.26	1	2.1×10 (1.8 meV)
Sn–SnO_2	No. 15	5230	0.3	1	1.8×10 (1.6 meV)
Sn–SnO_2	No. 40	8400	0.35	1	2.0×10 (1.7 meV)
Sn–SnO_2	No. 41	51500	0.82	1	2.2×10 (1.9 meV)
Sn–SnO_2	No. 12	6530	3.1	4[b]	8.8×10^5
Sn–SnO_2	No. 29	6380	3.6	4[b]	1.7×10^6
Sn–SnO_2	No. 14	4900	5.6	4[b]	2.2×10^6
Sn–SnO_2	No. 13	21200	9.9	4[b]	2.2×10^6
Sn–SnO_2	No. 18[c]	7850	20	4[b]	1.9×10^6
Sn–SnO_2	No. 31	15660	20	4[b]	6.2×10^6
Sn–SnO_2	No. 24	5300	45	4[b]	6.2×10^6
Sn–SnO_2	No. 39	260000	44	2	1.1×10^3
Sn–SnO_2	No. 37	65000	68.1	2	2.9×10^3
Sn–SnO_2	No. 36	8600	76.5	2	3.3×10^3
Sn–SnO_2	No. 38	5000	91	2	3.3×10^3
Sn–SnO_2	No. 34	94000	98.7	2	3×10^3
Sn–SnO_2	No. 32	12000	1500	1	2.9×10^2 (25 meV)
Sn–SnO_2	No. 46[a]	55000	1	2	3×10^3
Ta–Ta_2O_5	No. 2	19000	6.3	2	1.2×10^3
Ni–NiO	No. 6	20000	8.3×10^4	2	1.1×10^5

[a]Measured in the capacitance configuration.
[b]Attempt to fit with $n = 4$, although $n = 2$ is better fit.
[c]Deposited at 77 °K.

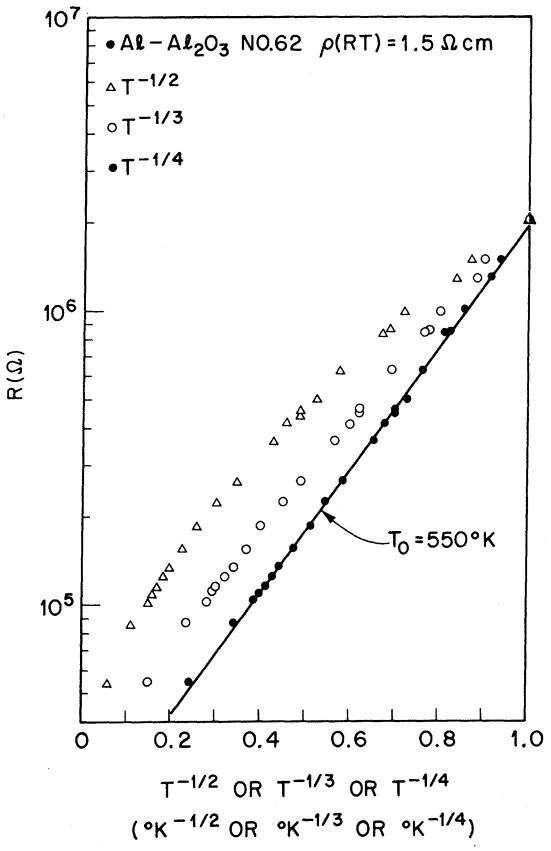

FIG. 2. Temperature dependence of the resistance fitted to $R = R_0\, e^{(T_0/T)^{1/n}}$ with $n = 2$, 3, 4 for an Al_2O_3 film with $\rho(\mathrm{RT}) = 1.5\ \Omega$ cm.

tion is still possible as long as the grains are weakly coupled, i. e., as long as the tunneling barrier between them is thin. As the Al_2O_3 content is further increased the grains become decoupled and a resistive transition can no longer occur. This point will be further discussed in conjunction with the susceptibility experiments.

The data shown in Fig. 1, which extend only over less than an order of magnitude in resistance, are rather well fitted by relation (1) with $T_0 = 43$ °K. The fit to relation (1) is much more convincingly established in Figs. 2 and 3. As the data were obtained down to 1 °K, Fig. 2 establishes convincingly that a fractional power of $\frac{1}{4}$ in relation (1) represents the best fit to the data. Although a straight line could be drawn through the $\frac{1}{3}$ power curve, a line that would be a good average for the data between 300 and 8 °K would clearly miss the 1 °K point; furthermore, a line drawn between the 300 °K point and the 1 °K point clearly reveals a downward curvature for the $\frac{1}{3}$ power curve which is further accentuated in the $\frac{1}{2}$ power curve. Furthermore, the same data were plotted in Fig. 3 on a log-log scale, and it is clear by the continuous curvature of the data that a power-law dependence of R on T can be ruled out. On the other hand, Chopra and Bahl[17] found that although the data on amorphous Ge were well represented by relation (1), "$R \propto T^{-7}$ provided an excellent fit for six decades of the variation of R over the temperature range 77–740 °K." It turns out, however, that this surprising outcome is the result of a fortuitous mathematical identify valid over the above-mentioned temperature range but not valid at all for $T \leq 10$ °K.[18] Consequently, whenever the data can be fitted by a relation similar to (1) below 10 °K (which is the case in the present study), one can rule out a power-law dependence. We shall now turn our attention to Al–Al_2O_3 films with increasing resistivities which can be described by the general equation

$$R = R_0\, e^{(T_0/T)^{1/n}}, \tag{2}$$

where the exponent n can take values between 1 and 4. In Fig. 4 one observes that films with room-temperature resistivities as high as 5. 5 Ωcm are well represented by relation (2) with $n = 4$ and a maximum value for T_0 of 10^5 °K. The fit is excellent between 77 and 1 °K, but it is obvious from Fig. 4 that the room-temperature point cannot be included. When $\rho(\mathrm{RT}) \simeq 10\ \Omega$cm the data can no longer be fitted with $n = 4$; indeed an excellent fit can be achieved with $n = 3$ for both the two-point- and four-point-contact method[19] as shown in Fig. 4. For higher resistivities (a few tens of Ωcm) the data can be fitted by relation (2) with $n = 2$ as shown in Fig. 5. Figure 5 shows again that the same temperature dependence is obtained whether the two-point-contact or the four-point-contact method is used. It is also clear from Table I and from Figs. 4 and 5 that for a given n value, the slope is steeper (i. e., T_0 is larger) the higher the room-temperature resistivity of the sample. The data for Al–Al_2O_3 No. 68 have also been plotted as a

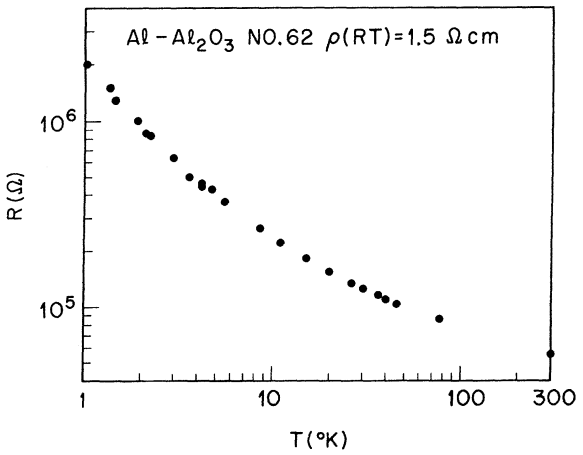

FIG. 3. Log-log plot of the data shown in Fig. 2.

function of $T^{-1/4}$ in Fig. 5, but no line was drawn through the data points so as not to prejudice the

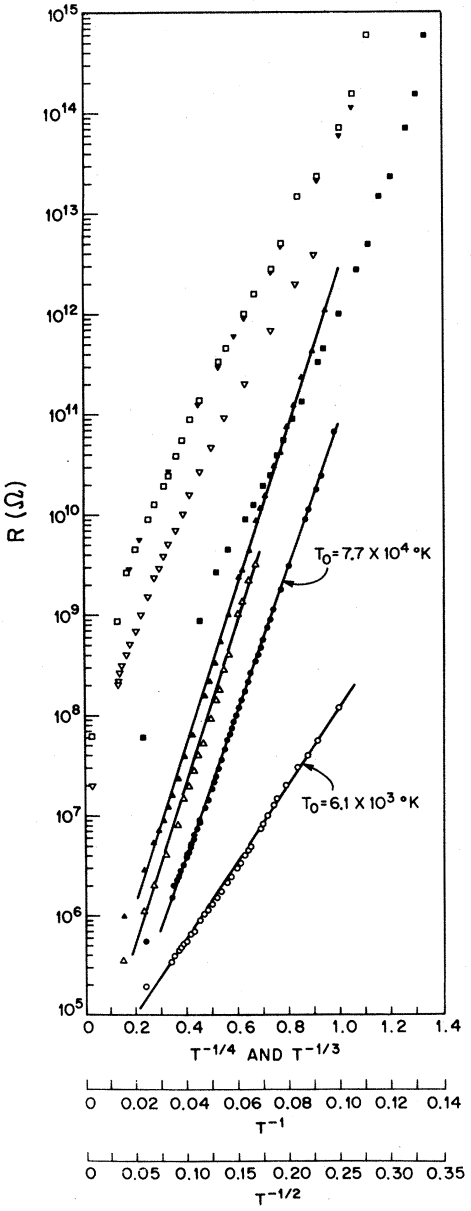

FIG. 4. Various temperature dependences of the resistance for Al–Al_2O_3 films ranging in room-temperature resistivities between 5 and 640 Ω cm. Open dot, Al–Al_2O_3 No. 60, $\rho = 5.05$ Ω cm, $T^{-1/4}$ scale four-point measurement; closed dot, Al–Al_2O_3 No. 65 $\rho = 5.5$ Ω cm, $T^{-1/4}$ scale two-point measurement; Al–Al_2O_3 No. 70, $\rho = 9.7$ Ω cm, closed triangle, $T^{-1/3}$ scale two-point measurement, open triangle, $T^{-1/3}$ scale four-point measurement; inverted open triangle, Al–Al_2O_3 No. 71, $\rho = 320$ Ω cm, T^{-1} scale; Al-Al_2O_3 No. 67 $\rho = 640$ Ω cm, closed square, $T^{-1/2}$ scale, open square, T^{-1} scale, inverted closed triangle, T^{-1} scale (current and voltage leads interchanged).

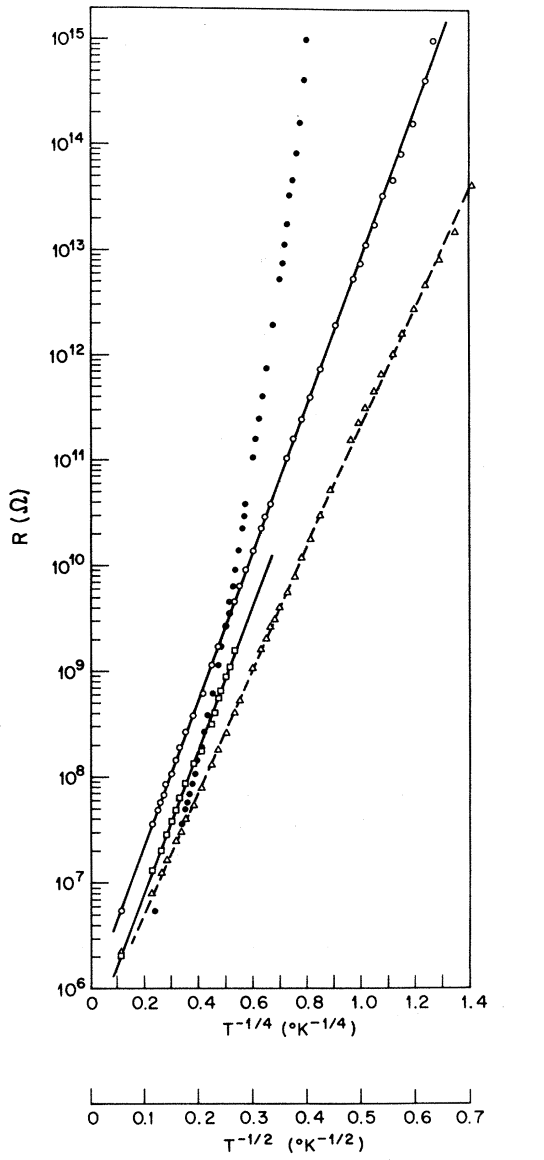

FIG. 5. Temperature dependence of the resistance for two Al–Al_2O_3 films with ρ(RT) = 17 and 35 Ω cm. Al–Al_2O_3 No. 68, $\rho = 35$ Ω cm, closed dot, $T^{-1/4}$ scale two-point measurement, open dot, $T^{-1/2}$ scale two-point measurement, open square, $T^{-1/2}$ scale four-point measurement; Al–Al_2O_3 No. 69, $\rho = 17$ Ω cm, open triangle $T^{-1/2}$ scale two-point measurement.

interpretation. These data points could be fitted with little error by a straight line between 77 and 10 °K and by a somewhat steeper line below 10 °K. It is, however, evident that the fit with $n = 2$ is much better and includes all the data down to 1 °K encompassing a change in resistance of eight decades. This brings one back to the general difficulty encountered in analyzing the conductivity of other amorphous materials, namely, the type of temperature dependence (exponential versus power

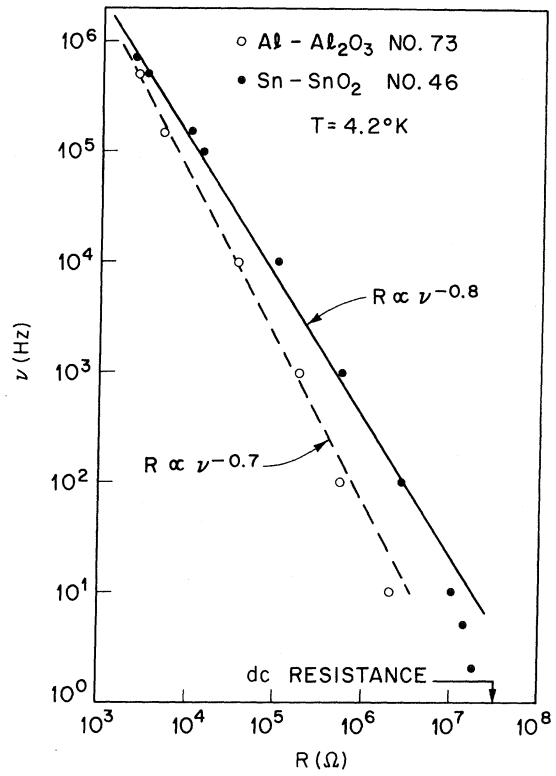

FIG. 6. Log frequency versus log resistance for an $Al-Al_2O_3$ film and a $Sn-SnO_2$ film both measured in the capacitance configuration between two gold electrodes.

law) and the numerical value of the exponents depend upon the range of data included in the analysis. The point was already suggested by Chopra *et al.*[17] in the case of amorphous Ge films and more recently by Morgan[20] who reported $T^{-1/4}$ characteristics below 8 °K and $T^{-1/3}$ between 8 and 50 °K in amorphous carbon films. Although different conductivity mechanisms[20] have been ascribed to the various characteristics, it is felt that this is a somewhat questionable procedure in view of experimental errors, and we have chosen instead to fit by a relation such as (2) with a single exponent the largest possible portion of available data. If one now considers films with the highest resistivities (a few hundreds of Ω cm) it can be seen from Fig. 4 that the temperature dependence is somewhat slower than a pure exponential ($n = 1$) but somewhat faster than that given by relation (2) with $n = 2$. Consequently, it seems that with increasing ρ(RT) (i.e., with increasing Al_2O_3 content) the temperature dependence of the resistance approaches a pure exponential. The data shown in Fig. 4 for $Al-Al_2O_3$ No. 67 with the inverted leads is an indication of the homogeneity of the films as the inversion of the leads results in measuring a different portion of the film without altering the data.

Films with room-temperature resistivity larger than $\simeq 1$ Ω cm are no longer superconducting by resistive measurements. Nevertheless, such films with resistivities as high as 320 Ω cm ($Al-Al_2O_3$ No. 71) become superconducting at 1.2 °K in a susceptibility measurement. The strength of the signal at 1.2 °K is quite weak and at best a few percent of the signal corresponding to the film being fully superconducting. This signal is too large to be explained by independent submicroscopic Al grains, as the shielding power of these particles would be at most 10^{-5} of the signal corresponding to a fully superconducting film. One can, however, explain the magnitude of this signal in two ways which are consistent with an essentially homogeneous film. Firstly, one can assume that the Al particles are close enough together (a few Å apart) to interact, so that their shielding power becomes larger than that of independent particles. On the other hand, the signal could also originate from either a few larger particles or loops of small connected particles which will lead to greater flux exclusion. Whatever the case may be, the superconducting susceptibility signal indicates the presence of some form of Al clusters and consequently, it is possible that submicroscopic clusters of size smaller than 20 Å may be present as well although they may not directly be inferred from the susceptibility measurements.

The ac resistance of an $Al-Al_2O_3$ film is shown as a function of frequency in Fig. 6. In this experiment the resistance of the film was measured between two gold electrodes. The temperature dependence of the dc resistance of this film followed relation (2) with $n = 3$. The data show that the ac resistance decreases with frequency as $\nu^{-0.7}$, which reflects a conduction by hopping[17]; the frequency exponent should be 1 for single hops and 0.5 for multiple hops. The dc dielectric constant of this film as determined from the capacitance measurement was 10.6 which is somewhat higher than the literature value for pure Al_2O_3 (8.4); this discrepancy could be due in part to the fact that the thickness of the film was certainly overestimated as a result of the non-steady-state character of the $Al-Al_2O_3$ sputtering.

The experimental results in the $Al-Al_2O_3$ system can therefore be summarized in the following manner: The temperature dependence of the resistance of all $Al-Al_2O_3$ films studied can be represented by relation (2) with $n = 4$ over a wide range of compositions. As shown in Table I, when the Al_2O_3 content is increased so that $\rho > 5$ Ω cm, the exponent n decreases progressively towards 1, which is the expected exponential behavior for a doped oxide. This behavior along with the ac results suggests that the conduction in such films is similar to the thermally activated hopping mechanism

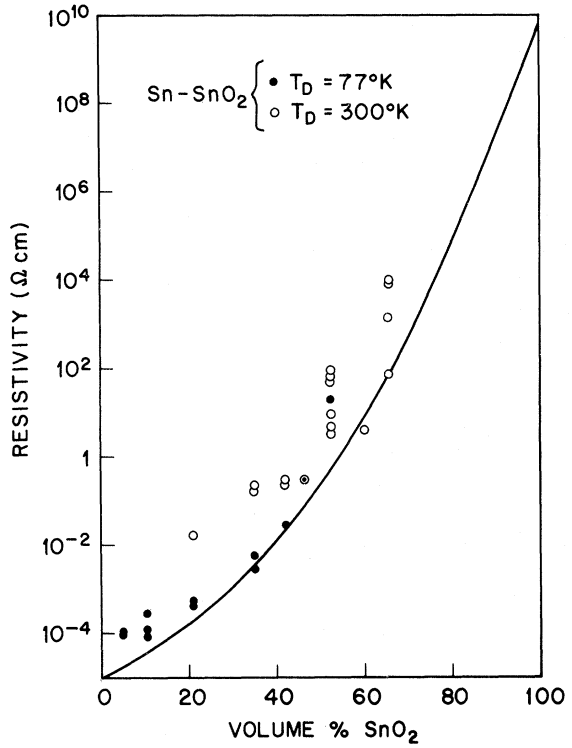

FIG. 7. Resistivity of Sn–SnO_2 films versus vol. % SnO_2. Some of the films were deposited at $T_D = 300$ °K and some at $T_D = 77$ °K. The solid line represents the average line drawn by Neugebauer (Ref. 2) for various cermet films versus vol. % SiO_2.

described for other amorphous materials.[7–11] The susceptibility experiments suggested the possible presence of submicroscopic Al clusters. If this were true, we would like to speculate that the energy levels could be quantized as a result of size quantization.[21] These energy levels could be the localized states between which the electrons hop. If one considers the quantized levels in a 20-Å-diam Al grain, such levels would be smeared by kT at about 80 °K,[21] thus explaining why the room-temperature data often seemed to deviate from the fitted curves. Although a hopping mechanism qualitatively explains the data, it seems very hard to reconcile the low observed values of T_0 with the percolation theory of Ambegaokar *et al.*[8] Their theoretical estimate of T_0 is given by

$$kT_0 = 16\alpha^3/\rho_0, \tag{3}$$

where α is the coefficient of exponential decay of the localized states and ρ_0 is the density of states at the Fermi level. In the case of amorphous Ge the experimental value for T_0 of 10^8 °K could be obtained from (3) with α in the range 10^7–10^8 cm^{-1} and $\rho_0 = 10^{19}$. Using the lowest possible value of α (10^7 cm^{-1}) and the maximum $\rho_0 \simeq 10^{22}$ yields a minimum value for T_0 of 2×10^4 °K. Consequently although this theory could explain in detail films with $\rho(\mathrm{RT}) > 5$ Ω cm, the parameters could not be adjusted to fit the films with the lower resistivities although as pointed out before, the experimental fit with $n = 4$ seems unquestionable for such films.

B. Sn–SnO_2

In contrast with the previous system, the sputtering of Sn–SnO_2 is a steady-state operation, i.e., the composition of the film is approximately that of the sputtering target. This claim is supported by the data shown in Fig. 7, where the room-temperature resistivity of the Sn–SnO_2 films can be obtained within one or two orders of magnitude from the volume concentration of SnO_2. Neugebauer[2] made a similar observation for metal/SiO_2 cermet films. The dispersion of the data shown in Fig. 7 is approximately the same as that shown by Neugebauer, who attributed it to different deposition conditions and substrate temperatures. Although he pointed out that one obtains a universal curve independent of the metal and only dependent on the oxide, it is interesting to observe that Neugebauer's curve for SiO_2 (solid line in Fig. 7) averages rather well the data obtained here on SnO_2. This result supports the claim made earlier on the Al–Al_2O_3 system that the room-temperature resistivity can be chosen as a measure of the oxide content of the film.

Sn–SnO_2 films with resistivities smaller than 1 Ω cm can be considered as quasiamorphous as the electron diffractions show broad diffuse rings. This is in contrast with Sn–SnO_2 films with $\rho > 1$ Ω cm, which, just like all Al–Al_2O_3 films, yield a totally diffuse electron diffraction pattern. The temperature dependence of the resistance for films with $\rho < 1$ Ω cm is shown in Fig. 8. Although the data below 7 °K can be fairly well represented by relation (2) with $n = 4$, it is clear that a pure exponential ($n = 1$) fits a much larger portion of the data (from 1.8 to 30 °K). The independence of this result on film thickness is demonstrated in Fig. 9 and Table I, where the exponential fit with an activation energy T_0 of about 2 meV is seen to hold for films as thick as 5 μm. All Sn–SnO_2 films with $\rho < 1$ Ω cm display, when measured by susceptibility, a superconducting transition around 3.8 °K. The relatively large strength of the superconducting signal indicates, in agreement with electron diffraction, that such films are granular with a grain size approximately 20 Å.

While Al–Al_2O_3 films displayed a superconducting transition for ρ as high as 320 Ω cm, Sn–SnO_2 films with $\rho > 1$ Ω cm show no sign of superconductivity at all. Consequently, such films are totally amorphous and could even be devoid of submicroscopic grains. This fact was confirmed by NMR measure-

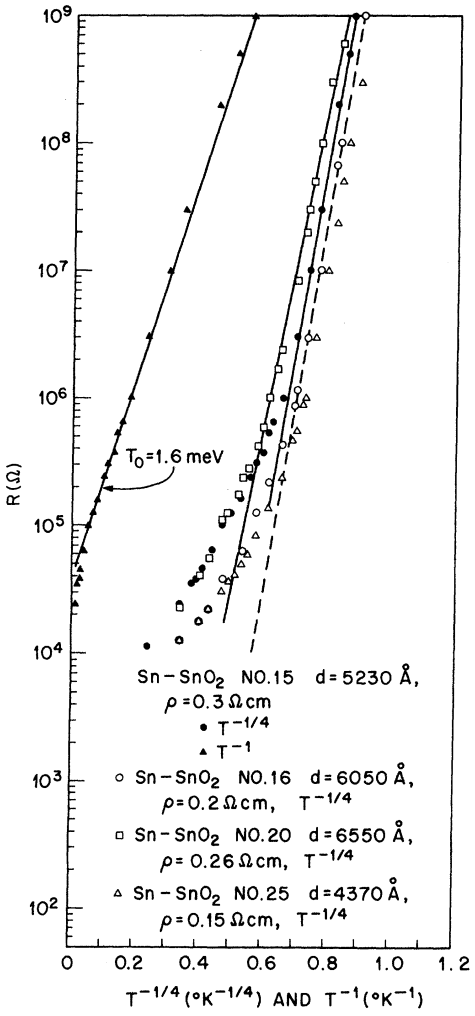

FIG. 8. Temperature dependence of the resistance for $Sn-SnO_2$ films deposited at 300 °K with $\rho < 1$ Ω cm.

ments[22] on a scraped 26-μm film ($\rho = 44$ Ω cm) which indicated a zero Knight shift. This does not exclude the possibility of a small concentration of Sn clusters containing a few Sn atoms, which could still behave as the localized states from which electrons can hop. The temperature dependence of the resistance for $Sn-SnO_2$ films with resistivities greater than 1 Ω cm is shown in Figs. 10–13 Figure 10 shows that an attempt to fit the data by relation (2) with $n = 4$ is certainly not bad over five decades change in resistance; one does, however, notice that the data display a slight positive curvature indicating a faster temperature dependence. This fact is clearly demonstrated in Fig. 11, where $n = 1, 2, 4$ has been attempted for $Sn-SnO_2$ No. 34 and clearly $n = 2$ is the best fit over eight orders of magnitude change in resistance. It is also clear from Figs. 10–12 that the fit with $n = 2$ is independent of thickness (d varies from 0.5 to 26 μm) and of the temperature of deposition (300–77 °K). One may notice in Fig. 12 a slight positive curvature for films No. 37 and No. 39. It is believed that such curvature may be caused by a small inhomogeneity in such thick films resulting from the very long time of deposition ($Sn-SnO_2$ No. 39 was deposited during three days). This assumption is supported by the annealing experiment performed on $Sn-SnO_2$ No. 38. As shown in Fig. 12, although the as deposited film is fitted very well by relation (2) with $n = 2$, the two-day anneal did result in a slight positive curvature. Finally, just like in the $Al-Al_2O_3$ system where one found that a pure exponential behavior ($n = 1$) is approached for high resistivities (high Al_2O_3 content), one observes an exponential dependence of R on T for $Sn-SnO_2$ films with $\rho \simeq 10^3$ Ω cm (Fig. 13). The activation energy of 25 meV is quite reasonable for conduction in a heavily doped oxide.

One may summarize these results by stating that the temperature dependence of the resistance of $Sn-SnO_2$ films can be well described by relation (2) with $n = 2$ for most of the films studied; n being 1 for both extremes, the metal-rich side or granular

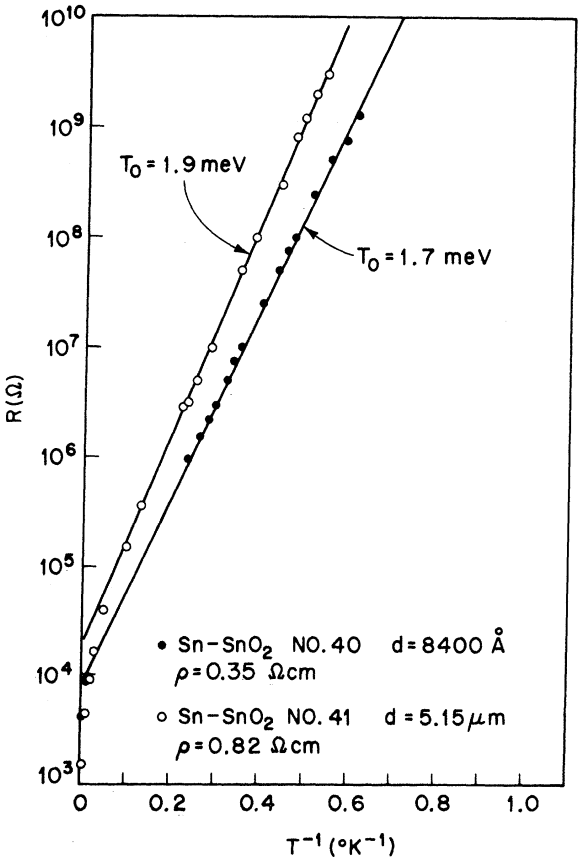

FIG. 9. $\text{Log}_{10}R$ versus $1/T$ for two $Sn-SnO_2$ films with $\rho < 1$ Ω cm deposited at 300 °K.

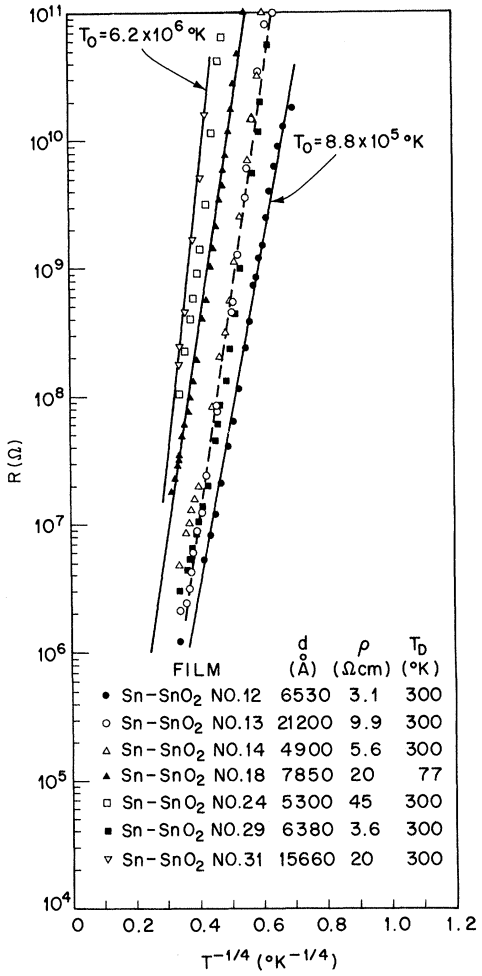

FIG. 10. $\text{Log}_{10}R$ versus $T^{-1/4}$ for Sn–SnO_2 films deposited at 300 and 77 °K (one film) with resistivities larger than 1 Ω cm.

films and the oxide-rich side or doped dielectric. The major difference in the Al–Al_2O_3 system is the absence of a region with $n=4$. This difference can be explained in terms of the different grain structure as a function of oxide content for the two systems, which in turn, may be the result of the different chemical activities of Al and Sn. In the case of the Al–Al_2O_3, as one increases the Al_2O_3 content the Al grain size decreases, but as suggested by the susceptibility measurements, there may be submicroscopic Al grains present almost up to the doped oxide limit ($\rho \simeq 1000$ Ωcm). This may result from the fact that when aluminum and oxygen are both present they always form either Al or Al_2O_3; there is neither a suboxide nor any appreciable solubility of oxygen in aluminum. On the other hand, up to 1 Ω, the Sn–SnO_2 system is still granular. If one increases the SnO_2 content beyond this point (i.e., more than 50-vol% SnO_2 as shown by Fig. 7) instead of the grain size diminishing further, grains disappear abruptly (even submicroscopic ones as suggested by susceptibility and NMR measurements). This may be explained by the fact that around 1 Ωcm, i.e., around the 50-50 volume concentration, Sn and oxygen will choose to form doped SnO rather than a mixture of Sn and SnO_2. We therefore attribute the absence of the $n=4$ region in the Sn–SnO_2 system to the absence of the submicroscopic Sn grains.

We now consider the measurement of a Sn–SnO_2 film in a capacitance configuration between two gold electrodes. The temperature dependence of the resistance for such a measurement is shown in Fig. 14. One may observe that the resistivity and the temperature dependence of the resistance ($n=2$

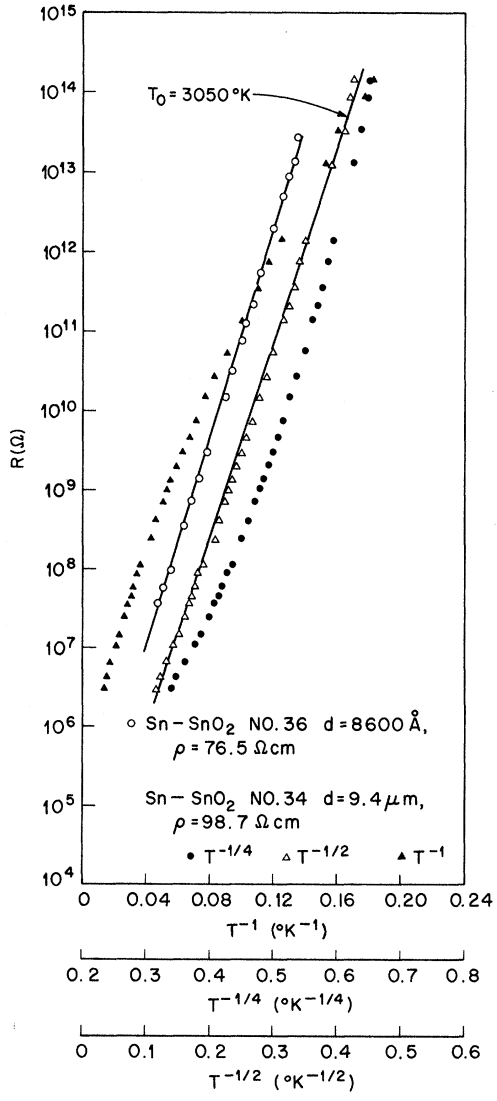

FIG. 11. Various temperature dependences of the resistance for Sn–SnO_2 films deposited at 300 °K.

and $T_0 = 3080$ °K) are in very good agreement with the measurements in a planar geometry (see, for example, Fig. 11). The ac resistance of this same film is shown in Fig. 6 as a function of frequency.

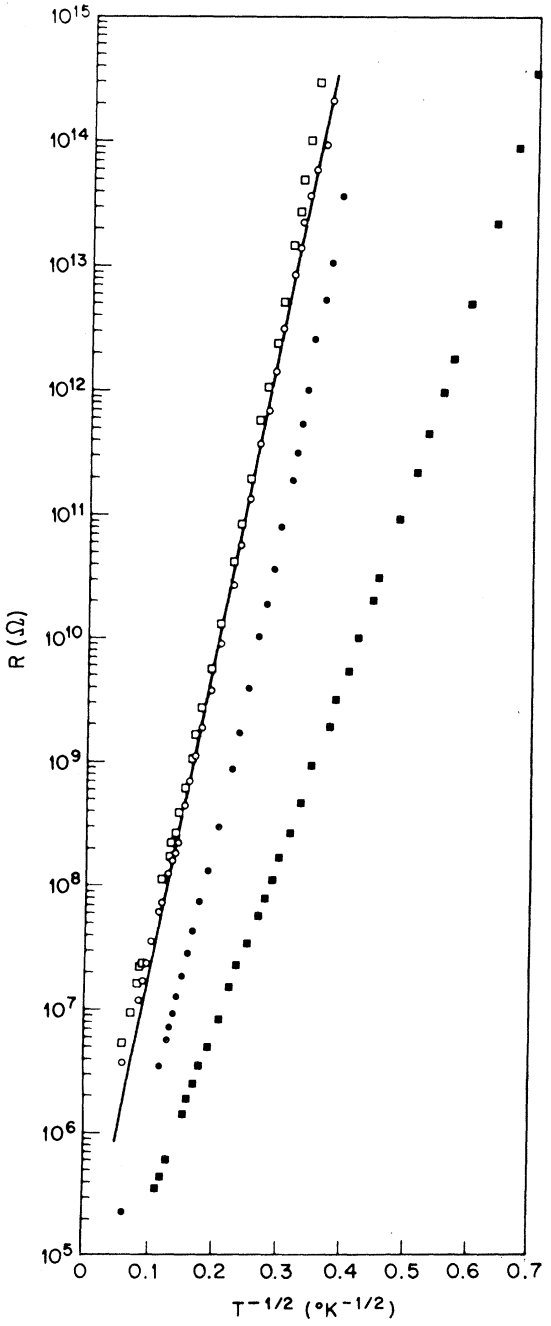

FIG. 12. Temperature dependence of the resistance for Sn–SnO_2 films deposited at 300 °K with $1 < \rho < 100$ Ω cm and $0.5 \leq d \leq 26$ μm. Closed dot, Sn–SnO_2 No. 37, $d = 6.5$ μm, $\rho = 68.1$ Ω cm; Sn–SnO_2 No. 38, $d = 5000$ Å, $\rho = 91$ Ω cm, open dot, as deposited, open square, after 2-day anneal at 300 °K; closed square, Sn–SnO_2 No. 39, $d = 26$ μm, $\rho = 44$ Ω cm.

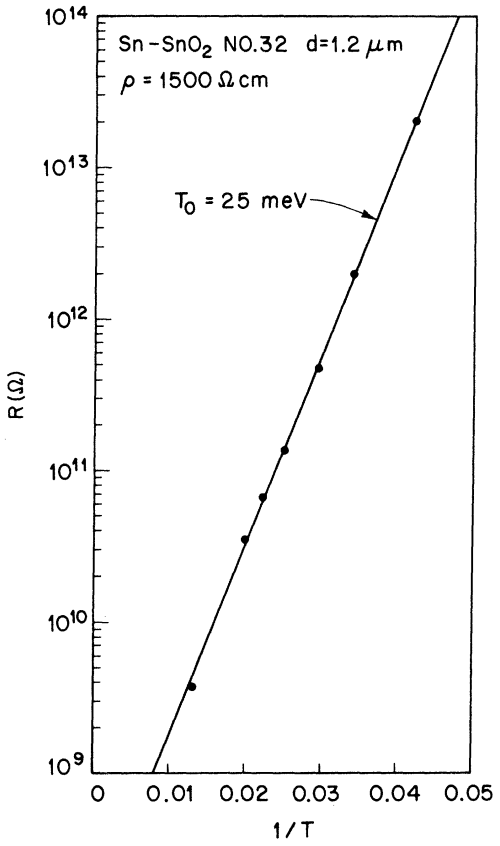

FIG. 13. $\text{Log}_{10}R$ versus $1/T$ for a Sn–SnO_2 film with $\rho = 1500$ Ω cm deposited at 300 °K.

The ac resistance decreases with frequency as $\nu^{-0.8}$, which is similar to the dependence found in many glasses[17,23] and corresponds to a hopping mechanism of conductivity. The voltage dependence of the current for the film discussed in Figs. 6 and 14 is shown in Fig. 15, and one can observe that at sufficiently high electric fields $\log_{10} I$ is a linear function of $V^{1/2}$. The deviation at low fields from the straight line is an indication that one is approaching an Ohmic behavior. In view of the experimental errors on the pertinent parameters, it is very hard to distinguish whether one is dealing at high electric fields with Schottky (S) or Poole–Frenkel (PF) emission.[17,24] In either case the current is given by[17]

$$I = AsT^2 e^{\beta E^{1/2} - e\Phi/kT}, \tag{4}$$

where A is the Richardson–Dushman constant, s is the active area, $\beta = \beta_S = \frac{1}{2}\beta_{PF} = (e^3/\epsilon)^{1/2}/kT$ with e the unit charge in esu and ϵ the high-frequency dielectric constant, Φ is the barrier height, and $E = V/d$ is the electric field due a voltage V applied across a thickness d. Consequently, according to relation (4) a plot of $\log_{10} I$ versus $E^{1/2}$ should be a

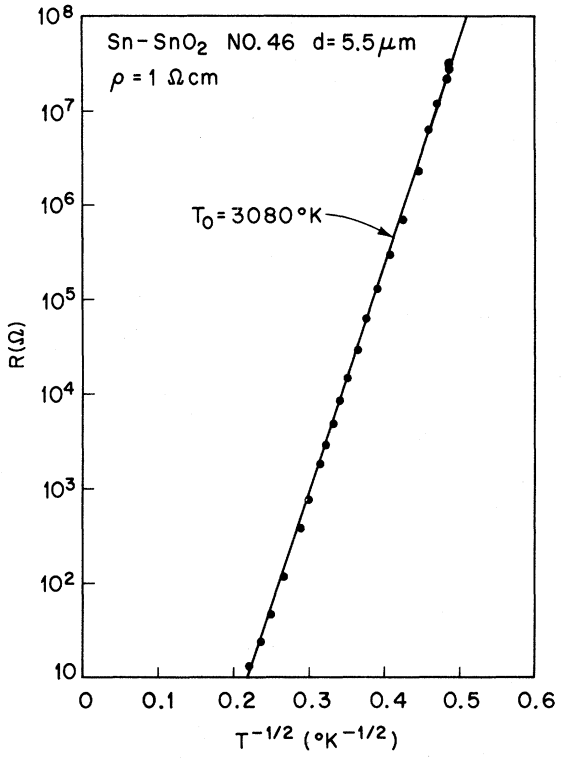

FIG. 14. Temperature dependence of the resistance for a Sn–SnO_2 film deposited at 300 °K and measured in the capacitance configuration between two gold electrodes.

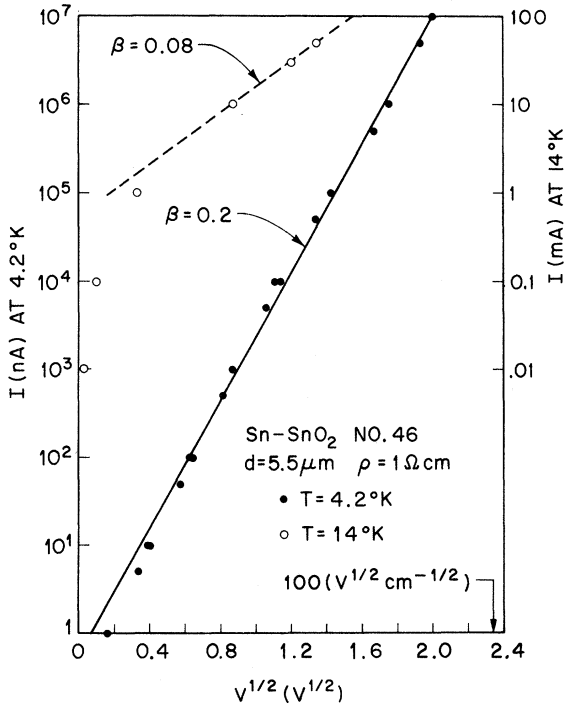

FIG. 15. Voltage dependence of the current measured at 4.2 and 14 °K in the capacitance configuration on the same Sn–SnO_2 film previously described in Figs. 6 and 14.

straight line with slope β. Using the experimental value of the dielectric constant determined by capacitance measurements ($\epsilon = 92$) one finds $\beta_{PF}(4.2\,^{\circ}\mathrm{K}) = 0.22$ and $\beta_{PF}(14\,^{\circ}\mathrm{K}) = 0.065$, which are in reasonable agreement with the respective experimental values of 0.2 and 0.08. One should also point out that similarly to amorphous Ge[10] there is an Ohmic region which extends at room temperature up to a few 1000 V/cm and which diminishes rapidly with decreasing temperature.

C. Ta–Ta_2O_5

We shall deal very briefly with this system and the next one as the results are essentially similar to those previously reported; it is, however, interesting to include them in order to stress the generality of the present results. Most films with thickness ranging from 0.4 to 5.2 μm and room-temperature resistivities ranging between 1 and a few 100 Ω cm can be represented by relation (2) with $n = 2$. This is shown on a typical film in Fig. 16, where the various temperature dependences have been explicitly attempted and $n = 2$ is clearly the best fit.

D. Ni–NiO

Films with thickness varying between 0.7 and 3 μm and room-temperature resistivities ranging

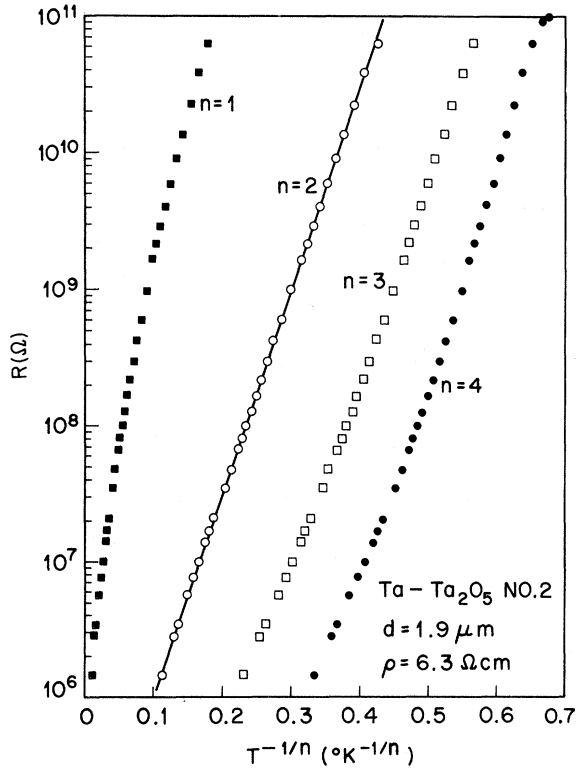

FIG. 16. Various temperature dependences of the resistance for a Ta–Ta_2O_5 film deposited at 300 °K.

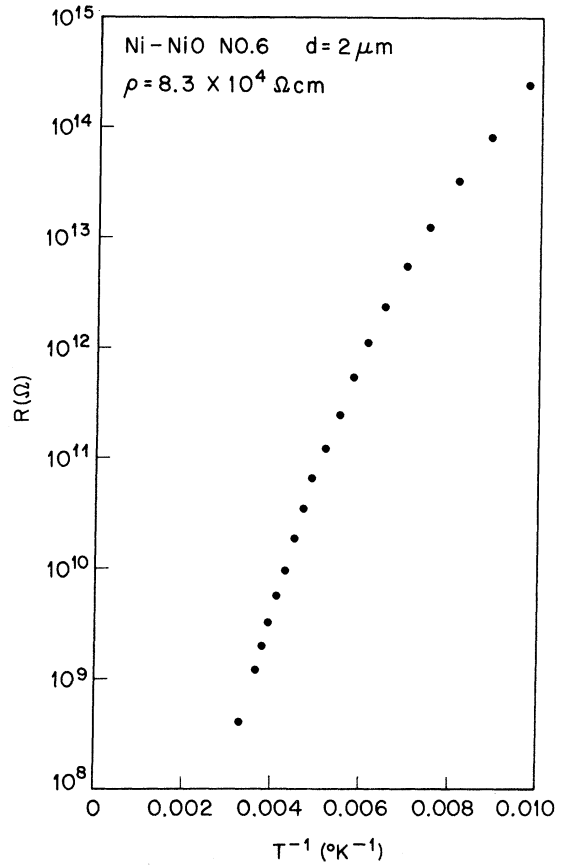

FIG. 17. $\text{Log}_{10}R$ versus $1/T$ for a Ni–NiO film deposited at 300 °K.

from 270 to 8.2×10^4 Ωcm are again well described by relation (2) with $n=2$. The temperature dependence of the resistance for the film with highest resistivity is shown in Fig. 17. In general, the activation energy at room temperature increases with increasing resistivity from 30 meV at $\rho=270$ Ωcm to 280 meV for $\rho=8.2\times10^4$ Ωcm. Furthermore, this activation energy decreases with decreasing temperature: For example, the 30-meV value decreases to 6 meV at 6 °K while the 280-meV activation energy decreases to 115 meV at 110 °K, as can be seen from Fig. 17. The results are in excellent agreement with Tsu *et al.*,[25] who reported an activation energy of 0.5 eV at 500 °K decreasing to 0.003 eV at 20 °K on an amorphous oxidized 50-Å Ni film.

IV. SUMMARY

In conclusion, these mixed amorphous metal–metal-oxide systems represent a large class of materials of which the electrical conduction is controlled by a temperature-dependent activation energy, the lowest activation energy occurring at the lowest temperature. This continuous distribution of activation energies coupled with the tunneling barriers result in a current of which the temperature, voltage, and frequency dependences are qualitatively similar to those previously described for other amorphous materials such as Ge and Si,[9–11,17] NiO,[13] C,[20] etc. The temperature dependence of the resistance is well represented by relation (2), with $n=2$ being the most general exponent. As shown in Table I, for a given n value, the slope is steeper (i.e., T_0 is larger) the higher the room-temperature resistivity of the sample. It is also obvious from Table I that for an average resistivity (around 10 Ωcm) the value of n (2) and of T_0 ($\simeq10^3$) is about the same for all systems studied (Al, Sn, and Ta).

Quite recently Gittleman *et al.*[26] reported on the magnetic properties of granular Ni–SiO_2 films. They showed a plot of $\log_{10}R$ versus $1/T$ with a monotonically decreasing activation energy, which they attempted to fit by a constant activation energy at the lowest temperature. Although this may be a borderline case for the present study since these films were not amorphous (grain size $\simeq$ 50 Å), it can be seen by Fig. 18 that most of the data below 77 °K are quite well fitted by relation (2) with $n=4$

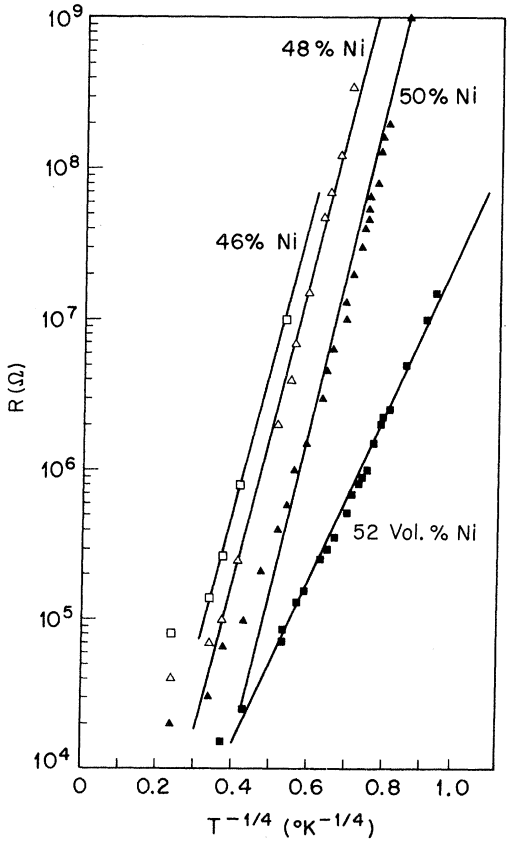

FIG. 18. Data plotted in Fig. 4 of Ref. 26 replotted here as $\log_{10}R$ vs $T^{-1/4}$.

(for some reason, the 50% Ni would be better fitted with $n=2$). One should also point out that Zeller,[27] who studied tunneling between small Sn particles embedded in Sn oxide, also reported a conductivity behavior which could be described by relation (2) with $n=2$. Finally, in the Al–Al_2O_3 system where relation (2) with $n=4$ seems to fit much of the data, it is difficult to reconcile the data with the theoretical parameters.

ACKNOWLEDGMENTS

The author would like to thank B. I. Halperin for helpful discussions and J. H. Wellendorf for his technical assistance.

[1]J. J. Hauser, Phys. Rev. B **3**, 1611 (1970), and the references to previous work cited therein.
[2]C. A. Neugebauer, Thin Solid Films **6**, 443 (1970).
[3]R. M. Hill, Proc. R. Soc. A **309**, 377 (1969).
[4]N. C. Miller, B. Hardiman, and G. A. Shirn, J. Appl. Phys. **41**, 1850 (1970).
[5]C. A. Neugebauer and M. B. Webb, J. Appl. Phys. **33**, 74 (1962).
[6]P. Sheng and B. Abeles, Phys. Rev. Lett. **28**, 34 (1972).
[7]N. F. Mott, J. Non-Cryst. Solids **1**, 1 (1968); Philos. Mag. **19**, 835 (1969).
[8]V. Ambegaokar, B. I. Halperin, and J. S. Langer, Phys. Rev. B **4**, 2612 (1971).
[9]P. A. Walley, Thin Solid Films **2**, 327 (1968).
[10]M. Morgan and P. A. Walley, Philos. Mag. **23**, 661 (1971).
[11]P. A. Walley and A. K. Jonscher, Thin Solid Films **1**, 367 (1968).
[12]I. G. Austin, J. Non-Cryst. Solids **2**, 474 (1970).
[13]I. G. Austin and N. F. Mott, Adv. Phys. **18**, 41 (1969).
[14]I. Z. Kostadinov, Zh. Eksp. Teor. Fiz. **14**, 345 (1971) [Sov. Phys.-JETP **14**, 231 (1971)].
[15]J. J. Hauser, J. Low Temp. Phys. **7**, 335 (1972).
[16]I am indebted to G. W. Kammlott for the electron diffractions.
[17]K. L. Chopra and S. K. Bahl, Phys. Rev. B **1**, 2545 (1970).
[18]The mathematical identity is that $\log_{10} T = 4 - 6.2\, T^{-1/4}$ with at most a 2.5% error for $80 \leq T \leq 800$.
[19]The two-point-contact method always gives a higher resistance value than the four-point-contact method because of the spreading resistance caused by the two-point contact geometry; the temperature dependence of the resistance is, however, identical in both measurements.
[20]M. Morgan, Thin Solid Films **7**, 313 (1971).
[21]A 20-Å-diam grain of Al contains 750 atoms which results in quantized levels approximately 7 meV apart.
[22]I am indebted to W. W. Warren for these NMR measurements.
[23]M. Pollak and G. E. Pike, Phys. Rev. Lett. **28**, 1449 (1972).
[24]K. A. Jonscher, Thin Solid Films **1**, 213 (1967).
[25]R. Tsu, L. Esaki, and R. Ludeke, Phys. Rev. Lett. **17**, 977 (1969).
[26]J. I. Gittleman, Y. Goldstein, and S. Bozowski, Phys. Rev. B **5**, 3609 (1972).
[27]H. R. Zeller, Phys. Rev. Lett. 28, 1452 (1972).

PHYSICAL REVIEW B VOLUME 7, NUMBER 9 1 MAY 1973

Dependence of the Thermal Conducitivity on the Direction of the Magnetic Field in Superconducting Films without Vortices*

P. Lindenfeld, R. D. McConnell,† and M. S. Moskowitz‡
Department of Physics, Rutgers University, New Brunswick, New Jersey 08903

(Received 6 November 1972)

We have measured the thermal conductivity of indium and indium-alloy films as a function of magnetic field, with the field direction in the plane of the specimen, both parallel and perpendicular to the heat flow. The films are either too pure or too thin to contain vortices. In films with short mean free path the thermal conductivity is less when the field is parallel to the heat current, in contrast to the situation when vortices are present. The magnitude of the anisotropy is consistent with calculations by Maki but the variation with magnetic field and with electronic mean free path is quite different.

INTRODUCTION

In this paper we describe an anisotropy of the thermal conductivity of superconductors in the absence of vortices. The effect is therefore different from that which has been observed previously in the mixed state of type-II superconductors.[1–3] It was discovered during the course of an investigation of a type-II alloy, when we were startled by the appearance of an anisotropy below the lower critical field opposite to that which is caused by vortex scattering.

Although the first reports appeared quite some time ago,[4,5] this is the first full description of our results. One reason for the delay is that the effect is small, and for unambiguous and detailed results we felt it necessary to construct a new apparatus and more precise instrumentation. Another reason is that the theoretical description continues to be beset with difficulties. An anisotropy like that described here is implicit in the discussion of Bogoliubov,[6] was calculated by